

Nanostructured zirconia layers as thermal barrier coatings

Sorina ILINA*¹, Gheorghe IONESCU¹, Victor MANOLIU²,
Radu Robert PITICESCU³

*Corresponding author

¹INCAS - National Institute for Aerospace Research “Elie Carafoli”
B-dul Iuliu Maniu 220, Bucharest 061126, Romania
sorinag@incas.ro

²Aerospace Consulting, B-dul Iuliu Maniu 220, Bucharest 061126, Romania

³National Institute of Research and Development for Non-Ferrous and Rare Metals
B-dul Biruinței 102, Pantelimon, Ilfov, C.P. 077145250, Romania
imnr@imnr.ro

DOI: 10.13111/2066-8201.2011.3.3.7

Abstract: *The coatings obtained by thermal spray are used both as antioxidant and connection materials (e.g. MCrAlY type alloys) as well as thermal barrier coatings (e.g. partially stabilized zirconia oxide with yttria oxide). This paper studies the characteristics of the coatings obtained with nanostructured powders by thermal spraying and air plasma jet metallization. Testing of coatings is done against the most disturbing factor, thermal shock. Structural changes occurring after thermal shock tests are highlighted by investigations of optical and electronic microscopy. The results obtained after quick thermal shock show a good morphological and surface behavior of the developed coatings.*

Key Words: 8YPSZ, AZY25, Al₂O₃, HVOF, APS, thermal shock.

1. INTRODUCTION

Classical ceramic for industry and the advanced ceramic for special applications (turbo engines, etc.) can now be considered, along with composite materials, the most often utilized material in different fields of technology. Ceramic thermal barrier coatings (TBC) have received increased attention as they are used for various applications ranging from heat overloaded components of gas turbines to turbine rotors and various components of the aircraft engine.

Among the economic benefits of their use the following should be mentioned: increased fuel efficiency and engine reliability improvement. The classic “recipe” of TBC systems is structured as follows: a ceramic insulator layer having a thickness of 120 ÷ 350 μm, known as top coat and a metallic layer (“bond coat”) with thickness values between 50 and 150 μm. These systems are known as the “duplex TBCs”.[1-3] Physically the coatings based on partially stabilized zirconia oxide with yttria oxide, as thermal barrier (TBC), has two major advantages: low thermal conductivity (2.2 ÷ 2.6 W/m¹K⁻¹ at room temperature) and a relatively high coefficient of thermal expansion (10⁻⁶/°C).[1] The zirconium properties which give the material a thermal barrier role are: resistance to temperatures above 2400°C, high density, low thermal conductivity, chemical stability, wear resistance, high hardness; etc. *These properties are transferred to the resulting products.*

Since 1997 the use of nanostructured powders based on zirconia oxide for thermal barrier coatings was developed at global level.

These led to improved physical properties of the system and increased wear resistance of materials. A significant reduction in grain size in the case of nanomaterials induces an increase in resistance to thermal fatigue by an average of 170°C, as compared to conventional materials.[1, 4] The most widely used methods for deposition of YSZ are: Electron Beam Physical Vapor Deposition (EB-PVD) and Atmospheric Plasma Spraying (APS). The APS deposition method allows high quality coatings with low thermal conductivity and lower processing costs as compared to EB-PVD technique. [4]

Also, the structural link formed between the ceramic and the metal layer by APS deposition allows to obtain adherent layers, with a dense and smooth structure, and a thickness between 0.2 ÷ 3 mm depending on the type of application.

To improve the TBC layers the development of structures which have as component the aluminum oxide layers to increase resistance to oxidation of the material were taken into account [5-6].

In this paper we comparatively studied the thermal shock behavior and structural changes of ceramic layers based on nanostructured zirconia powder partially stabilized with yttrium oxide with and without Al₂O₃.

2. MATERIALS AND METHODS

There have been achieved three types of coatings with different concentrations of aluminum oxide. As metal substrate an alloy of nickel-chromium-cobalt, NIMONIC 90 was used. Physical properties are: density: 8.18 g/cm³, melting point: 1310°C, electrical resistivity at 20°C, 118 μΩcm, having high tensile strength and creep resistance at high temperatures up to about 950°C.

Ceramic coatings were obtained by air plasma spray coating APS and the bonding layers by High Velocity Oxy Fuel (HVOF).

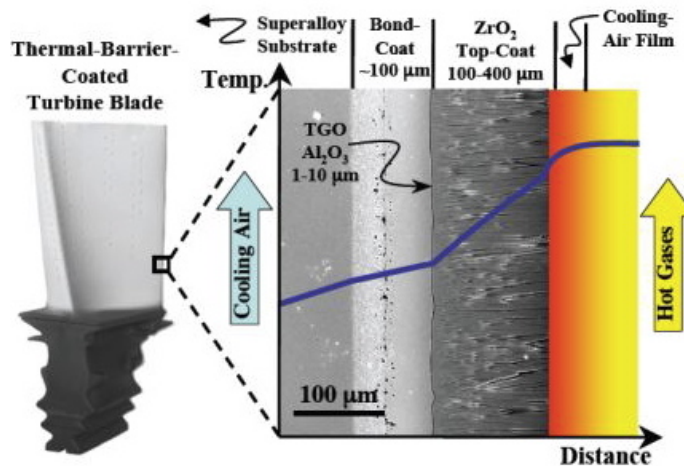


Fig. 1 Schematic of a thermal barrier system for applications in gas turbines (Padture et. al. Science, 2002)

Powders utilized to produce thermal protective coatings are presented below. For ceramic layers of samples numbered 1 ÷ 3 were used zirconia oxide powder partially stabilized with 7% yttria oxide (7YPSZ) and for the specimen number 4 we utilized nanostructured powder of ZrO₂-Y₂O₃-Al₂O₃ synthesized by hydrothermal obtained from National Institute of Research and Development for Non-Ferrous and Rare Metals - IMNR, Romania [7]. The chemical composition of the ceramic powder is: 75% ZrO₂ stabilized with

4 mol% Y_2O_3 + 25% Al_2O_3 . Other physical characteristics of the powder: crystallite size (XRD-Scherer) 8.1 nm, grain size (after counseling and granular) of less than 150 μm ; natural slope angle $46^{\circ}10'$; 28s/50g rate of flowing (STAS 8651-88) through the cone having the orifice diameter of 3 mm and apparent density of 1.69 g/cm^3 .

Powder METCO 204NS-AP, Fig. 2, has spheroid morphology (particle size: $-106 + 16 \mu m$), chemical homogeneity, structural stability and high purity.

For all the specimens Amdry 997 powder was used as bond coat; chemical composition: Ni 23Co 20Cr 8.5Al 0.6Y 4Ta.

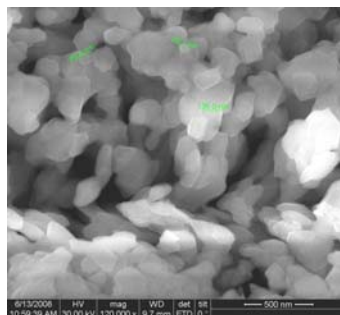


Fig. 2 Nanometric zirconia particles (x120000)

The layers of ceramic specimens numbered from 1 ÷ 3, Table 1, were coated with a variety of compositions based on partially stabilized zirconia. The choosing of the aluminum oxide as bonding layer or component in YPSZ to highlight the effect of oxidation YPSZ and aluminum oxide influence on the mechanism of delamination. Technological parameters of air plasma spray are: 7MB plasma jet torch, *deposition distance* 60 - 70 mm, Ar 80/H₂ 15, electric arc 500 A, U=60–65 V, Carrier 37. The structure of the samples, the material and the thickness of coatings are given in Table 1.

3. DISCUSSION

3.1 THERMAL SHOCK TESTS

Tests were conducted using QTS2 installation of quick thermal test shock (Fig. 3) conceived and achieved by INCAS laboratories. Thermal shock testing involves performing cycles of heating, maintaining and cooling of the specimen. The temperatures at which these tests were performed are the following: 900°C, 1000°C, 1100°C, 1150°C and 1200°C. For each temperature 25 cycling, with a time of heating and maintaining in the oven for 5 min and air cooling for 1 min were performed in automatic mode.



Fig. 3 QTS2 Quick thermal test shock installation

QTS 2 functional parameters:

- Maximum testing temperatures 1500°C
- The heating-cooling speed of the specimen is dependent on the number of layers, material thickness, composition, density, microstructure and the design of test installation. The average heating speeds obtained experimentally on QTS2 are 12° C/s and average cooling rates are 38°C/s for TBC specimen. The thermal shock is higher at cooling.
- Functional parameters monitoring
- Quick and continuous measurement of specimen and oven temperatures
- Data acquisition system with Lab View software.

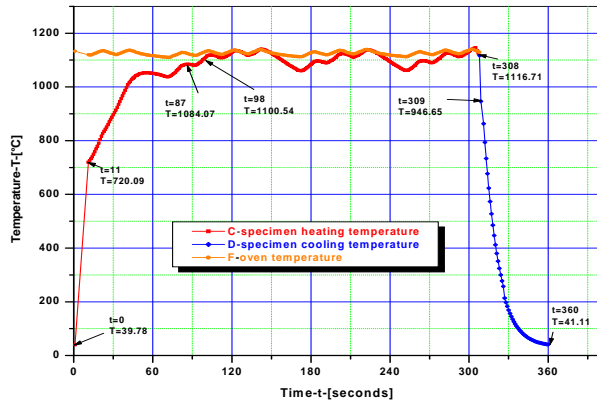


Fig. 4 Heating- cooling curve - Nimonic 90/MeCrAlY/ ZrO₂Y₂O₃Al₂O₃ specimen; testing temperature 1100°C

Fig. 4 shows the thermal shock test of the specimen Nimonic 90/MeCrAlY/ ZrO₂Y₂O₃Al₂O₃ at 1100°C. It highlights the rapid heating and cooling rates when the specimen is introduced and removed from the oven; the rates reduce when the regime temperature (1100°C) or ambient temperature is achieved. The parameters monitoring and data acquisition was performed by a data acquisition system and Lab View software that allowed real-time working.

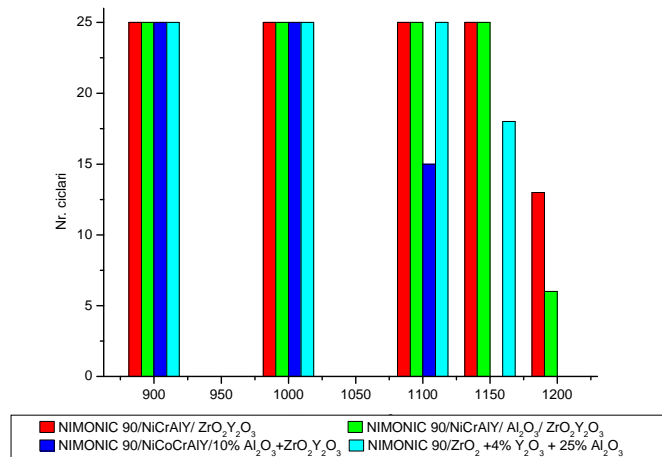


Fig. 5 Thermal cycling test results of nanostructured TBCs

Thermal shock test results are influenced by the layer thickness, phase constituents, deposition temperature and roughness of ceramic surface [6-7]. The maximum temperature at which the tests were conducted exceeded 1100°C. Results from Fig. 6, the layers deposited with ceramic powder $ZrO_2Y_2O_3Al_2O_3$ have poor thermal shock behavior; the maximum testing temperature was 1150°C as compared to ceramic layers obtained from YPSZ powder for which the maximum temperature was 1200°C.

3.2 INVESTIGATION OF ELECTRONIC AND OPTICAL MICROSCOPY

Electronic microscopy investigations were performed with scanning electron microscopes of SEM - JXA 50A and SEM-EDAX type (JXA - JEOL).

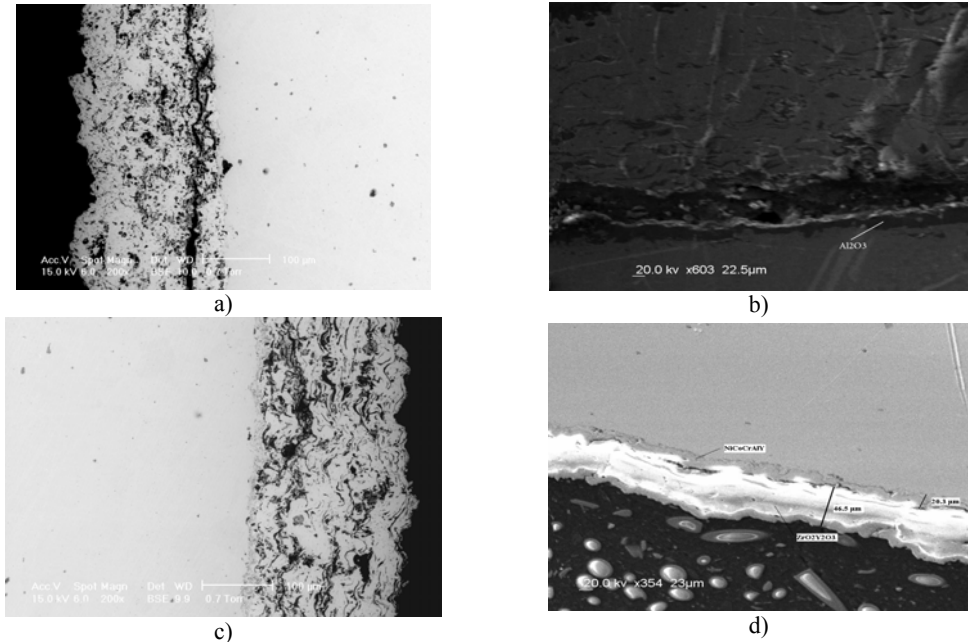


Fig. 6 SEM image of composition before the thermal shock test:
 a) NiCrAlY/ $ZrO_2Y_2O_3$ (x2608) ; b) NiCrAlY/ Al_2O_3 / $ZrO_2Y_2O_3$, (x603);
 c) NiCoCrAlY/ $Al_2O_3+ZrO_2Y_2O_3$ (200x); d) NiCrAlY/ $ZrO_2Y_2O_3Al_2O_3$ (x354)

The YPSZ ceramic layers have in the bonding layer filiform formations located along the substrate with a composition similar to the mass base of the substrate. The ceramic layer is adherent even if it has micro voids formed during deposition. The thickness is between 200µm and 250µm with an average of 222µm. The bonding layer has a thickness of 45µm and it adheres to the super alloy support. (Fig. 6a) The test specimen 2, NIMONIC 90/NiCrAlY/ Al_2O_3 / $ZrO_2Y_2O_3$ shows at the bonding layer-ceramic interface a layer with high proportion of aluminum oxide due to Al_2O_3 interlayer. The bonding layer with a thickness between 8 and 15µm is compact and very well anchored on the metallic surface. The coating contains up to 36.18% Zr in the mass basis and has thread-like structure formation with a composition close to the oxide layer. Ceramic coating shows relatively low porosity. The stratified layered morphology is the cause of reticular horizontal cracks formation in the layer. (Fig. 6b) Specimens 3 and 4, NIMONIC/NiCoCrAlY/ $ZrO_2Y_2O_3Al_2O_3$, present inside the ceramic layer filiform formations that extend along this layer following the substrate surface morphology. In their composition the aluminum oxide concentration was found to be double as compared to that of the base layer. The bonding

layer has a thickness of up to $20\mu\text{m}$. The ceramic layer thickness is between $47\mu\text{m}$ and $64\mu\text{m}$. At the bond coat/base metal interface the presence of horizontal cracks can be observed. (Fig. 6 c) and d))

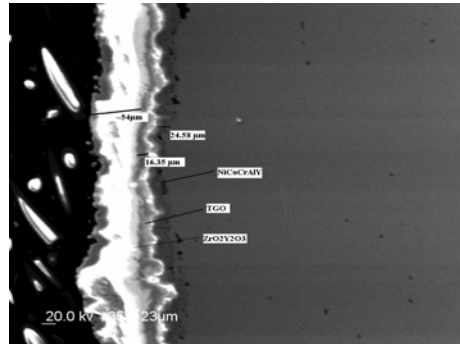


Fig. 7 SEM image of composition after the thermal shock test at 900°C

Electron microscopy investigations carried out after testing the samples at a temperature of 900°C reveals that at the bonding/ ceramic layer interface a transitional oxide layer has been formed, TGO - thermal oxide grown with a variable thickness ranging between $15.69 - 16.35\mu\text{m}$. This oxide layer was formed after the migration of reactive components from this layer (e.g. Al). The preservation of ceramic coating thickness uniformity can be noticed. The ceramic layer thickness ranges between $47 \div 64\mu\text{m}$ and that of the bonding layer between $17.65 \div 24.58 \mu\text{m}$. At the bonding layer/base metal interface horizontal cracks can be observed.

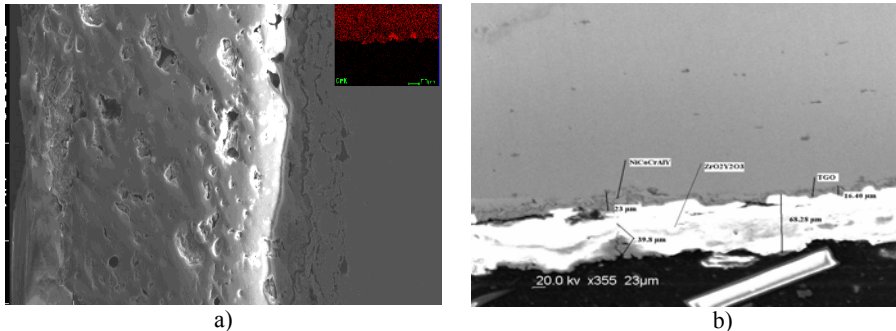


Fig. 8 SEM image of composition after the thermal shock test at 1000°C :
a) NiCrAlY/ $\text{ZrO}_2\text{Y}_2\text{O}_3$ (x400); b) NiCrAlY/ $\text{ZrO}_2\text{Y}_2\text{O}_3\text{Al}_2\text{O}_3$ (x355)

Secondary electron image obtained on the sample number 1 reveals a porous zirconia layer and a bonding layer thickness of $30\text{-}40 \mu\text{m}$ (Fig 8a). In Fig. 8 a), from upper right Cr-rich agglomerations in the bonding layer and multiple formations rich in aluminum and oxygen can be noticed. NiCrAlY/ $\text{ZrO}_2\text{Y}_2\text{O}_3\text{Al}_2\text{O}_3$ coated specimen, Fig. 8b shows a uniformity of the ceramic layer thickness ($46.5\text{-}55\mu\text{m}$). The bonding layer thickness is of $17\text{-}21.6\mu\text{m}$. At the bonding layer/base metal interface as well as at the bonding layer/ceramic layer interface some horizontal cracks can be observed. After 1000°C there is a change in the thickness of the observed layers.

The ceramic layer thickness is $68.28\mu\text{m}$ and that of the bonding layer is $23\mu\text{m}$. At the bonding layer / ceramic layer interface there is a TGO layer - thermal oxide grown with a variable thickness between $5.69 - 16.40\mu\text{m}$.

Table 1 Types of powders used, the thickness of layers, cycling temperature and test cycles number

Specimen code	Deposited layers	Layer thickness (mm)	Test temperature/ number of tests
1-N 56	NiCrAlY/ ZrO ₂ 7%Y ₂ O ₃	0.05/0.2	900/1000/1100/1200 (25/25/25/13)
2-N 27	NiCrAlY/Al ₂ O ₃ / ZrO ₂ 8%Y ₂ O ₃	0.05/0.05/ 0.2	900/1000/1100/1200 (25/25/25/6)
3-N22	NiCoCrAlY/10%Al ₂ O ₃ +ZrO ₂ 8%Y ₂ O ₃	0.05/0.2	900/1000/1100 (25/25/15)
4-N 96	NiCoCrAlY/ZrO ₂ + 4% Y ₂ O ₃ +25% Al ₂ O ₃	0.05/0.1	900/1000/1100/1150 (25/25/25/18)

CONCLUSIONS

Coatings studied in this paper show good characteristics in terms of thermal shock resistance and morphology of layers.

- Thermal barrier coatings systems were obtained from nanostructured zirconia powder partially stabilized with yttria with / without aluminum oxide

- Maximum temperature at which the tests were conducted exceeded 1200°C. For specimens deposited with nanopowder NiCrAlY/ZrO₂Y₂O₃Al₂O₃ the ceramic layer deteriorates in most areas, but the bonding layer remains adherent. In remote areas there is the possibility of detachment of the bonding layer due to the porosity and reticular cracks.

- Formation of oxide layer at the bonding layer / ceramic layer interface is due to migration of reactive elements from the bonding layer, their oxidation by chemical reactions at high temperatures, and aluminum oxide. The formation of these oxides, especially Al₂O₃, causes cracks at the bonding layer / ceramic layer interface due to stress-induced by transformation of γ - alumina in α -alumina.

REFERENCES

- [1] G. Moskal, *Thermal barrier coatings: characteristics of microstructure and properties, generation and directions of development of bond*, Journal of Achievements in Materials and Manufacturing Engineering, Volume 37 Issue 2, December 2009.
- [2] R. C. Tucker, *Thermal Spray Coatings, Metals Hand-book, Vol. 5: Surface Engineering*, ASM International, 497-509, 1993.
- [3] S. Bose and J. DeMasi-Marcin, *J. Therm. Spray Tech-nol*, **6**, 99, 1997.
- [4] S. M. Meier, D. K. Gupta, *The evolution of thermal barrier coatings in gas turbine applications*, Journal of Engineering for Gas Turbines and Power **116**, 250-257, 1994.
- [5] A. G. Evans, D. R. Mumm, J. W. Hutchinson, G. H. Meier and F. S. Pettit, *Prog. Mater. Sci.*, **46**, 505, 2001.
- [6] J. H. Sun, E. Chang, C. H. Chao and M. J. Cheng, *Oxidation of Metals*, **40**, 465, 1993.
- [7] <http://www.cnmp.ro:8083/pncdi2/program4/documente/2010/sedinta/rez/D7/72179.pdf>.
- [8] Y. C. Tsui and T. W. Clyne, in *Thermal Spray: Practical Solutions for Engineering Problems*, C. C. Berndt, ed. (ASM International, Materials Park, OH, 1996), pp. 275–284.
- [9] M. Gell, L. Xie, E. H. Jordan, N. P. Padture, *Surf. Coat. Technol.* **188–189**, 101–106, 2004.
- [10] K. W. Schlichting, N. P. Padture, E. H. Jordan, M. Gell, *Failure modes in plasma-sprayed thermal barrier coatings*, Materials Science and Engineering A, **342** (1/2), 120–130, 2003.
- [11] B. Liang, C. X. Ding, *Thermal shock resistances of nanostructured and conventional zirconia coatings deposited by atmospheric spraying*, Surface and Coatings Technology, **197** (2/3), 185–192, 2005.
- [12] A. Nusair Khan, J. Lu, *Behavior of air plasma sprayed thermal barrier coatings subject to intense thermal cycling*, Surface and Coatings Technology, **166** (1), 37–43, 2003.
- [13] A. Nusair Khan, J. Lu, *Thermal cyclic behavior of air plasma sprayed thermal barrier coatings sprayed on stainless steel substrates*, Surface and Coatings Technology, **201** (8), 4653–4658, 2007.